eJSSNT Superexpress Letter

e-Journal of Surface Science and Nanotechnology **21**, 128−131 (2023)

Classification of EBSD Kikuchi Patterns for Stainless Steel by Unsupervised Learning Methods to Investigate Grain Boundaries

Satoka Aoyagi,[a, †] Daisuke Hayashi,[a] Yoshiharu Murase,[b] Naoya Miyauchi,[b] Akiko N. Itakura [b]

[a] *Faculty of Science and Technology, Seikei University, 3-3-1 Kitamachi, Kichijoji, Musashino, Tokyo180-8633, Japan*
[b] *National Institute for Materials Science, 1-2-1 Sengen, Tsukuba, Ibaraki 305-0047, Japan*
[†] *Corresponding author: aoyagi@st.seikei.ac.jp*

Received: 20 January, 2023; Accepted: 20 February, 2023; J-STAGE Advance Publication; 25 February, 2023; Published: 25 February, 2023

Electron backscatter diffraction (EBSD) indexing based on Kikuchi diffraction patterns, which indicate the types and orientation of the crystal lattice, is effective for characterizing crystals. Most regions in a sample can be indexed due to simulation of diffraction patterns of possible crystal types, orientations, and angles. However, indexing some of the complex regions related to the grain boundaries, dislocations, and strain areas is difficult. Moreover, minor crystal structures are possibly omitted from the index results. To characterize all the regions, including such complicated boundaries, the analysis of raw data, including all Kikuchi patterns, is necessary. By analyzing all the Kikuchi patterns, significant information can be extracted from mixed crystal conditions. Stainless steel was used as the model sample in this study. As hydrogen diffusion in metals strongly depends on the crystal structure and grain boundaries, structural analysis is required to study hydrogen behavior in steel. In this study, all Kikuchi patterns at all pixels in a measurement area of stainless steel were analyzed simultaneously using unsupervised learning methods, such as principal component analysis and multivariate curve resolution, and the pixels of the measurement area were classified based on the Kikuchi patterns to investigate the grain boundaries and dislocations in detail.

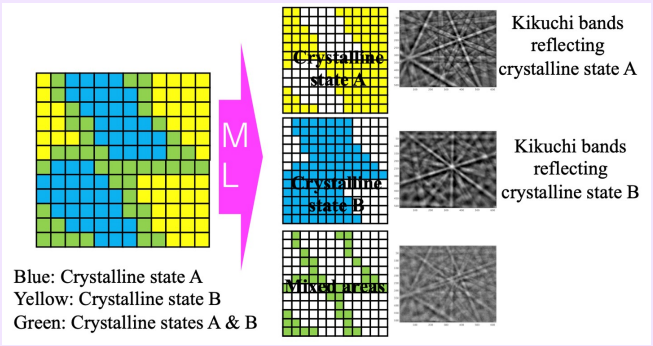

Keywords *Electron backscatter diffraction; Kikuchi bands; Principal component analysis; Multivariate curve resolution; Steel*

I. INTRODUCTION

The electron backscatter diffraction (EBSD) technique detects the electron diffraction pattern, called Kikuchi bands [1, 2], which reflects the crystalline state, such as crystal structures and orientation, at the measured point where the electron beam interacts with the sample [1]. EBSD provides detailed crystalline information, determines the crystal structure and orientation, discriminates different phases, and indicates grain boundaries. EBSD results contain significant information on the crystal condition of a sample. A detailed description related to the boundaries and disorder of complex crystals is generally indicated by specific maps such as the grain orientation spread map, grain average misorientation map, and Kernel average misorientation (KAM) map. Separate analysis processes are required to obtain such maps; therefore, the information is provided only if an analyst intentionally looks for such information. The analysis method based on all Kikuchi band patterns provides information without specific purposes. Moreover, distortion caused by unknown factors can also be found.

In our previous studies on hydrogen diffusion in stainless steel [3−5], the hydrogen distribution on the stainless steel surface and EBSD data were integrated to evaluate the relationship between the crystal conditions and hydrogen diffusion, as EBSD is a powerful tool to investigate detailed crystal structures [1, 2, 6−10] in inorganic materials and metals such as stainless steel. The stainless steel model is

composed of grains with face-centered cubic (fcc) and body-centered cubic (bcc) crystal structures. A detailed evaluation of the raw EBSD data is required to investigate the grain boundaries, dislocations, and areas of strain. Since EBSD analysis software, such as AZtecCrystal processing software (Oxford Instruments KK) and OIM analysis (TSL Solutions Ltd.), provides Kikuchi patterns for various materials by simulating diffraction patterns depending on the crystal type, orientation, and angle, most of the regions can be indexed. However, indexing regions related to the boundaries between different crystal conditions is complex, and thus, minor crystal structures can possibly get omitted. Therefore, all Kikuchi patterns over the measured areas were analyzed using unsupervised learning methods, such as principal component analysis (PCA) and multivariate curve resolution (MCR). MCR has been used for extracting pure spectra from a mixed spectrum [11−13]. Thus, it will also be useful for separating each Kikuchi band set associated with a pure crystal.

II. METHODS

A. Stainless steel sample analysis with EBSD

The model sample was austenitic stainless steel (SUS304) with dislocations produced by cold working [3−5]. The sample thickness was 100 μm, and the grain size was 50−150 μm.

The sample surface was polished using a cross-sectional polisher (IB-19520CCP, JEOL Ltd.) with an accelerating voltage of 3 kV. The sample was analyzed using EBSD (Symmetry, Oxford Instruments) with a scanning electron microscope (SU3500, Hitachi High Tech Corp.). The accelerating voltage was 20 kV, the step size was 1 μm, and the raster size was 74 × 82 μm^2.

B. EBSD data analysis by PCA and MCR

The measured area of EBSD contained 6068 (= 74 × 82) images of the Kikuchi pattern comprising 512 × 622 pixels. The EBSD Kikuchi pattern dataset was analyzed by PCA and MCR using the PLS toolbox (Eigenvector Research Inc.) and MATLAB (MathWorks) [11−13]. The detailed procedures are shown in the supplementary material.

III. RESULTS AND DISCUSSION

Typical EBSD images, such as Euler angles and the IPF map, of the samples are shown in Figure 1(a, b). Figure 1(b) indicates that the measured area of the sample was mainly composed of austenite with the fcc crystal structure. In areas A, B, C, and D in Figure 1(a), different orientations indicated by the Euler angles were mixed. The distortion of the sample can be evaluated by the maps provided by EBSD, such as the grain orientation spread map, grain average misorientation map, and KAM map in Figure 1(c), which indicates distortion-related regions.

In this study, the 74 × 82 pixels of the measurement area were considered as variables, and the 512 × 622 pixels in the Kikuchi patterns were considered as samples for PCA and MCR (the details are shown in Supplementary Material). Therefore, the score images of PCA and concentration matrix images of MCR show Kikuchi patterns and loadings of PCA, and the spectrum matrix of MCR shows sample images, as shown in Figure 2. The principal component (PC) contribution rates were PC 1 (89.10%), PC 2 (0.72%), PC 3 (0.58%), PC 4 (0.33%), PC 5 (0.26%), PC 6 (0.20%), PC 7 (0.16%), PC 8 (0.14%), and PC 9 (0.13%), and the residual components contained 8.39% information. Because the steel sample predominantly consists of austenite (fcc), PC1, most information from the raw data, represented austenite information. The other PCs mainly exhibited crystal orientation differences in the measurement area. Regarding the loading images, PC2 was consistent with the dark orange areas of the Euler angle image and the light blue areas of the IPF map, whereas PC3 represented the blue areas of the Euler angle image and the purple areas of the IPF map. The information size of PC4 and the PCs that were smaller than PC4 was too small to be considered.

In terms of MCR, each component (C in Figure 2) had a

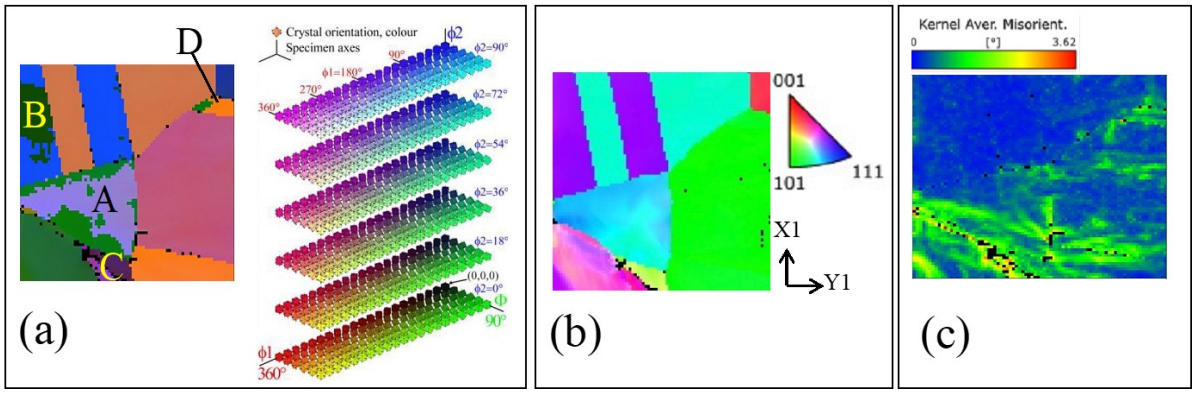

Figure 1: EBSD data of crystal information. (a) Euler angle images; colors of Euler angle images: red (Φ1) 0°−360°; green (Φ) 0°−90°; and blue (Φ2) 0°−90°. (b) Inverse pole figure (IPF) map; colors of IPF maps: red fcc [001]; green fcc [101]; and blue fcc [111]. (c) Kernel average misorientation (KAM) map. The field of view is 74 × 82 μm^2.

relatively large contribution rate. Components 1−10 contained 16.15%, 13.91%, 11.27%, 10.80%, 10.03%, 7.75%, 7.08%, 5.15%, 4.76%, and 4.82% information, respectively, and the residual components contained 8.28% information. Some components extracted by MCR indicated information not shown in the main EBSD results, such as Euler angle images and IPF maps. Components 2 and 3 (C2 and C3) showed similar Kikuchi patterns and sample distributions as PC2 and were mainly related to fcc [101], as shown in the IPF map of fcc [101] (Figure S4 in Supplementary Material). In addition, the brightest areas of C2 and C3 were different, which suggests a slight difference in the crystal conditions in these areas. Both the IPF map (Figure S4) and the Euler angle images did not show such significant information. C4 and C6 also showed similar Kikuchi patterns, even though their brightest areas differed. These are also related to fcc [101] because their bright areas are included in the IPF map of fcc [101] shown in Figure S4 (Supplementary Material). The Kikuchi patterns of C2 and C3 and those of C4 and C6 contained the same Kikuchi bands but with different angles.

The boundaries indicated by C8 are related to the KAM image shown in Figure 1(c) and Figure S5 (Supplementary Material). The Kikuchi pattern of C8 (concentration matrix of C8) may be a combination of other Kikuchi patterns, such as the C5 and C9 patterns. Although the main crystal structure information provided by EBSD analysis software is useful, extracting information related to the boundaries or disorder of the crystals is still challenging. The analysis of all Kikuchi patterns across the measurement area effectively extracted such minor but critical information.

IV. CONCLUSIONS

To characterize complex crystal conditions such as grain boundaries and dislocations in a solid sample, the analysis of all Kikuchi patterns over the EBSD measured area proved useful. By analyzing the Kikuchi patterns using unsupervised learning methods such as PCA and MCR, detailed information related to the boundaries and disorder of complex crystals that was not indicated by the conventional analysis based on main crystal orientations was extracted. Moreover, the complete Kikuchi pattern analysis enabled the extraction of each crystal condition in the region with multiple crystal conditions.

Acknowledgments

The authors would like to thank Drs. Hideaki Miyashige and Makoto Ikarashi from Oxford Instruments for measuring the model sample with EBSD. This work was partly supported by JSPS KAKENHI (Grant no. 18H03849, Japan).

Appendix

EBSD data analysis procedures by PCA and MCR is available in Supplementary Material at https://doi.org/10.1380/ejssnt.2023-023.

References

[1] A. J. Schwartz, M. Kumar, B. L. Adams, and D. P. Field (Eds.), *Electron Backscatter Diffraction in Materials Science*, 2nd ed. (Springer, New York, 2009).

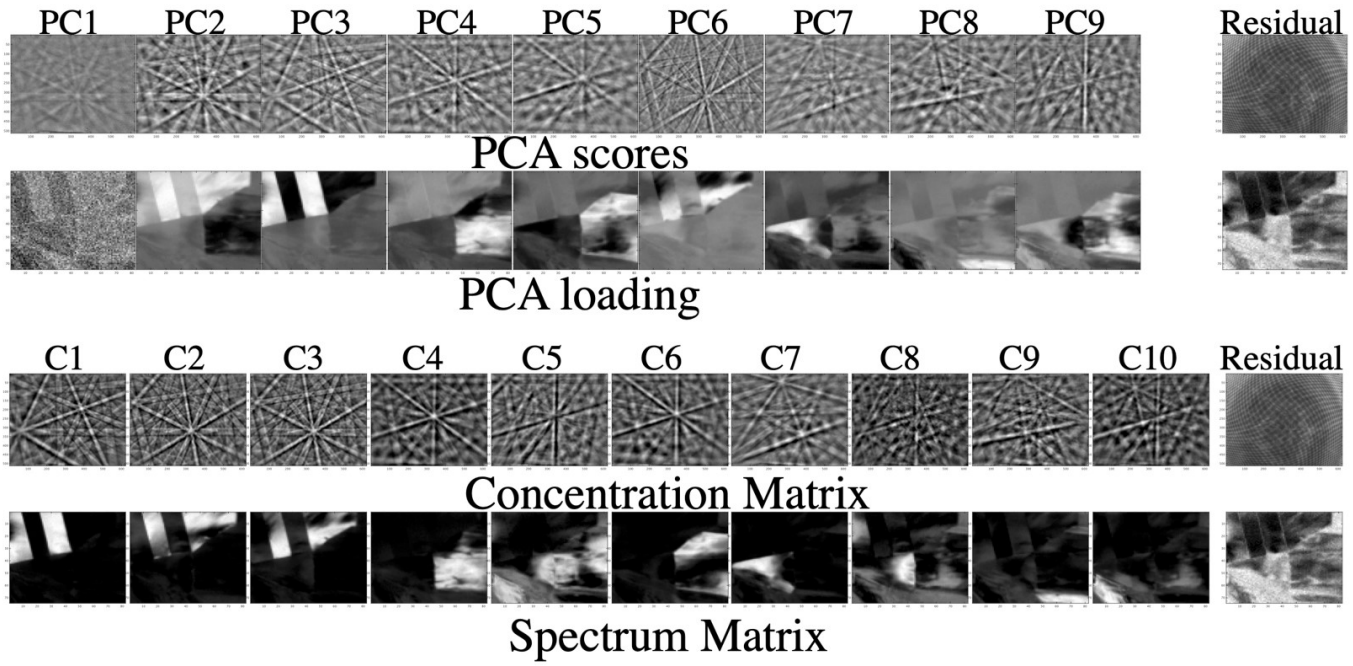

Figure 2: PCA results (scores and loadings) and MCR results (concentration matrix and spectrum matrix). PC stands for the principal component of PCA and C stands for the component of MCR. The residual images of PCA and MCR show the remaining data after PCA or MCR.

[2] A. Winkelmann, G. Cios, T. Tokarski, G. Nolze, R. Hielscher, and T. Kozieł, Acta Mater. **188**, 376 (2020).
[3] N. Miyauchi, T. Iwasawa, Y. Murase, T. Yakabe, M. Kitajima, S. Takagi, T. Akiyama, S. Aoyagi, and A. N. Itakura, Appl. Surf. Sci. **527**, 146710 (2020).
[4] T. Akiyama, N. Miyauchi, A. N. Itakura, T. Yamagishi, and S. Aoyagi, J. Vac. Sci. Technol. B **38**, 034007 (2020).
[5] A. N. Itakura, N. Miyauchi, Y. Murase, T. Yakabe, M. Kitajima, and S. Aoyagi, Sci. Rep. **11**, 8553 (2021).
[6] G. Nolze, A. Winkelmann, and A. P. Boyle, Ultramicroscopy **160**, 146 (2016).
[7] W. C. Lenthe, L. Germain, M. R. Chini, N. Gey, and M. De Graef, Acta Mater. **188**, 579 (2020).
[8] T. Tanaka and A. J. Wilkinson, Ultramicroscopy **202**, 87 (2019).
[9] K. Hata, M. Wakita, K. Fujiwara, K. Kawano, T. Tomida, M. Sugiyama, T. Fukuda, and T. Kakeshita, Mater. Trans. **57**, 1514 (2016).
[10] A. E. Davis, X. Zeng, R. Thomas, J. R. Kennedy, J. Donoghue, A. Gholinia, P. B. Prangnell, and J. Q. Da Fonseca, Mater. Charact. **194**, 112371 (2022).
[11] S. Aoyagi, T. Matsuzaki, M. Takahashi, Y. Sakurai, and M. Kudo, Surf. Interface Anal. **44**, 772 (2012).
[12] Y. Yokoyama, T. Kawashima, M. Ohkawa, H. Iwai, and S. Aoyagi, Surf. Interface Anal. **47**, 439 (2014).
[13] T. Kawashima, T. Aoki, Y. Taniike, and S. Aoyagi, Biointerphases **15**, 031013 (2020).